The catabolism of alanine and glutamate ensure proper sporulation by preventing premature germination and providing energy sources respectively

Fengzhi Lyu[1], Tianyu Zhang[1], Dong Yang[1], Meng Gui[2], Yongtao Wang[1], Xiaojun Liao[1], Lei Rao[1]

[1] College of Food Science and Nutritional Engineering
National Engineering Research Center for Fruit and Vegetable Processing
Key Laboratory of Fruit and Vegetable Processing of Ministry of Agriculture and Rural Affairs
Beijing Key Laboratory for Food Non-Thermal Processing
China Agricultural University
Beijing, China

[2] Beijing Fisheries Research Institute
Beijing Academy of Agriculture and Forestry Sciences
Beijing, China

Correspondence
Lei Rao, College of Food Science and Nutritional Engineering, China Agricultural University, 100083, Beijing, China
Email: rao.lei@cau.edu.cn

ABSTRACT

Sporulation as a typical bacterial differentiation process has been studied for decades, and the morphological events along with the molecular regulation mechanisms are relatively clear. However, two other important aspects of sporulation, (i) how sporulating cells gain energy sources to fuel sporulation proceeding, and (ii) how generated spores maintain dormancy during the whole sporulation process lack research. Here, we found that RocG-mediated glutamate metabolism was crucial for driving mother cell lysis to succeed sporulation, likely by providing energy metabolites ATP. Interestingly, high-level rocG expression generated excessively high ATP contents in sporulating cells, which caused adverse effects on the properties of the future spores, e.g. faster germination efficiency, lower DPA content along with decreased heat resistance. Moreover, we revealed that Ald-mediated alanine metabolism decreased the typical germinant L-alanine concentration to a certain level in the sporulating environment, thus avoiding premature germination and maintaining spore dormancy. Our data inferred that sporulation was a highly orchestrated and exquisite biological process requiring the balance of diverse metabolism pathways, hence ensuring both the sporulation completion and the high quality of generated spores.

INTRODUCTION

Spores are formed by bacteria belonging to the orders *Bacillales* and *Clostridiales* in response to unfavorable environmental conditions such as nutrient limitation (1, 2). Spores are metabolically dormant and considered as the most resilient living organisms due to their extreme resistance to harsh environment and can exist for even millions of years (3-5). The process of forming spores from bacterial vegetative cells is termed sporulation. Taking the model bacterium *Bacillus subtilis* as an example, the morphological process of sporulation can be divided into several stages, including asymmetric division, engulfment, spore maturation, mother cell lysis and spore release (6). Specifically, as vegetative cells commit themselves to sporulation, the earliest visible event is the asymmetric division, producing the septum to divide the vegetative cell into a larger mother cell and a smaller forespore. Subsequently, the mother cell membrane migrates around the forespore until it is completely enclosed. This phagocytosis-like process is identified as engulfment. At this time, the double-membrane structure of forespore forms, followed by the cortex synthesis and spore coat assembly. Then, the forespore chromosomes are saturated with small acid-soluble proteins (SASPs), and the water in the forespore is replaced by DPA synthesized in the mother cell, leading to forespore dehydration. These events lead to the appearance of phase-bright spores. Next, mother cell lysis occurs after spore maturation, allowing the spores to be released into the environment.

Research on the morphological events of the sporulation process, as well as the underlying gene expression and molecular mechanisms, has been continued for decades (6-10). However, relative few research focuses on how to guarantee proper sporulation, especially the quantity and quality of spores. When referred to proper sporulation, we essentially indicate two aspects. The first one is the normal progression of the sporulation event. Since sporulation

is considered as an energy-consuming biological process (11), the energy supply is critical to promote the progress of the sporulation event. Studies have speculated that amino acid metabolism, such as glutamate and alanine metabolism, are potential energy sources that drive sporulation (12-14). However, their regulatory mechanisms during sporulation remain unclear. The second aspect is that the spores should remain dormant during the whole sporulating process. Although depletion of nutrients in the environment is a prerequisite for sporulation initiation (15), quantities of factors that induce germination still exist around generated spores. How the spores keep dormant in that tempting environment remains a mystery to be explored. Previous research has reported that the deletion of *ylbJ*, *pdaB*, or SpoVA protein encoding genes led to the loss of dormancy maintaining ability, as these mutants exhibited premature germination during sporulation (16, 17). The reasons for premature germination are diverse, including inappropriate activation of germination receptors, incorrect assembly of spore outer structure, and deficiency in the SpoVA channel. Hence, defects in any aspect will lead to abnormal sporulation and adversely affect the quantity or quality of spores produced. However, the precise mechanism of how spore maintain dormancy during sporulation is still unclear.

Here, we reported that the RocG-mediated glutamate metabolism played a crucial role in ensuring proper sporulation, especially promoting the mother cell lysis, by providing energy sources. We also found that high level *rocG* expression caused excessively high ATP contents in sporulating cells, which adversely affected the properties of the correspondingly generated spores, including faster germination efficiency, lower DPA content along with decreased heat resistance. Moreover, we also revealed that the Ald-mediated alanine metabolism decreased the concentration of the typical germinant L-alanine in sporulating environment to a certain level, thus avoiding premature germination and maintaining spore dormancy.

RESULTS

Proteins regulating alanine, aspartate and glutamate metabolism are enriched by proteomics analysis during sporulation of *B. subtilis*

In order to explore the metabolic pathways crucial for *B. subtilis* sporulation, Tandem Mass Tag-based (TMT) quantitative proteomics analysis was carried out between dormant spores (DS) and sporulating vegetative cells (VC) at t_0 (Figure 1A). Hierarchical clustering analysis (HCA) was conducted to exhibit the overall differences of protein expression between DS and VC group (Figure 1B). Greater differences between groups were showed in the HCA heatmap than that within groups, indicating that the protein expression in DS and VC was significantly different. The differentially-expressed proteins were screened with the criteria $p < 0.05$ and fold change > 1.2 (the expression level increased by more than 1.2-fold or decreased by less than 0.83-fold). 1,259 proteins with increased expression as well as 1,248 proteins with deceased expression were screened out in VC group (Figure 1C). KEGG pathway enrichment analysis of these differently expressed proteins revealed the great changes in several metabolism between DS and VC groups, including alanine, aspartate and glutamate metabolism, ribosome, flagellar assembly, glyoxylate and dicarboxylate metabolism, and methane metabolism (Figure 1D). Among these pathways, the most significant changes were identified in alanine, aspartate and glutamate metabolism, suggesting their crucial roles in the sporulation of *B. subtilis*. Previous studies have indicated that *ald*, encoding alanine dehydrogenase Ald, and *rocG*, encoding glutamate dehydrogenase RocG, are crucial regulators of alanine and glutamate metabolism, respectively (13, 18). In addition, Δ*ald* and Δ*rocG* mutants have been verified to exhibit remarkable sporulation deficiency (13, 14). However, the deletion of *ansB* gene, encoding L-aspartase important for aspartate metabolism, has no significant effect on sporulation (19). Hence, the effects of alanine and glutamate metabolism on

sporulation were further explored in this work.

Alanine and glutamate metabolism co-regulate sporulation with an additive effect

Since alanine and glutamate metabolism have been reported separately to be involved in sporulation (13, 14, 20), we wonder if these two pathways can jointly affect the sporulation process. To verify this hypothesis, we constructed Δ*ald* Δ*rocG* mutant and observed that significant fewer phase-bright spores were produced in the double mutant strain than in Δ*ald* or Δ*rocG* mutants (Figure 2A). This result indicated that the sporulation defect of Δ*ald* Δ*rocG* mutant was more significant than that of Δ*ald* or Δ*rocG* mutants. This was further demonstrated by examining the heat-resistant spores produced in sporulation, as the percentage of Δ*ald* and Δ*rocG* spores was 10.9% and 29.8% respectively, while Δ*ald* Δ*rocG* mutant was only 0.3% (Figure 2B). The severe sporulation deficiency of Δ*ald* Δ*rocG* mutant suggested that Ald and RocG co-regulated sporulation in an additive effect. Moreover, quantities of phase-dark forespores were observed in Δ*ald* Δ*rocG* mutant (Figure 2A), which could be attributed to two reasons including (i) limited energy sources supporting the sporulation proceeding, or (ii) premature germination caused by abnormal spore structure assembly or inappropriate in-situ sporulating environment (16). We then deleted *gerAA* to investigate if premature germination occurred in Δ*ald* Δ*rocG* mutant. As shown in Figure 3A, the sporulation defect of the double mutant was partially rescued, as 29.7% of phase-bright spores formed in Δ*ald* Δ*rocG* Δ*gerAA* (Δ3) mutant, indicating that premature germination indeed existed. However, the only partial rescue effect suggested that premature germination was not the exclusive reason of the sporulation defect in Δ*ald* Δ*rocG* mutant. Hence, the limitation of energy support can still be a substantial explanation of sporulation defect phenotype of the double mutant strain. We then explored these two possibilities in the following work.

RocG-mediated glutamate metabolism, but not Ald-mediated alanine metabolism, is essential for ensuring the sporulation efficiency and the spore quality likely through energy supply

As the Ald and RocG mediated alanine and glutamate metabolisms were proposed as potential energy sources for sporulation (13, 14), we speculated that these two metabolic pathways provided energy support separately. If this was the case, excessive complementation of either metabolism pathway should be able to rescue the sporulation defect of the Δ*ald* Δ*rocG* mutant. Here, we used Δ*ald* Δ*rocG* Δ*gerAA* (Δ3) strain to exclude the premature germination effect and independently explored the energy supply mechanism in this part (Figure 3A). Based on this, *ald* and *rocG* were artificially expressed separately and jointly in Δ3 under IPTG-inducible promoter. Results showed that elevating the expression level of *ald* by increasing the concentration of IPTG up to 5 mM had no significant effect on the quantity of phase-bright spores in Δ3 mutant, with the sporulation percentage between 20% and 30% (Figure S1, Figure S2A). Accordingly, these spores showed significant germination deficiency under AGFK induction (Figure S2B, Figure 3C). However, the elevated *rocG* expression level upon addition of at least 10 mM IPTG restored the sporulation of Δ3 mutant to 53.4%, similar with that of wild-type (56.8%) (Figure 3B). Moreover, when more than 20 mM IPTG was added, the germination deficiency of Δ3 mutant spores was recovered to the level of wild-type (Figure S2B, Figure 3C). Notably, Δ3 mutant with IPTG-induced *ald* and *rocG* co-expression showed the same sporulation and germination phenotypes as that with IPTG-induced *rocG* sole expression (Figure S2B, Figure 3C). Hence, in Δ3 mutant, the sole complementation of RocG succeeded to rescue the sporulation defect, but not the case for that of Ald. This indicated that RocG-mediated glutamate metabolism appeared to regulate sporulation by providing energy sources whereas Ald-mediated alanine metabolism may not play the same role.

To further explore if these two catabolism pathways are involved in controlling the spore quality, mutants of transcription factors of Ald and RocG, Δ*adeR* and Δ*ahrC* Δ*rocR* (14, 21), were respectively constructed to test the germination phenotype of the spores. *gerAA* was also knocked out in these mutants to ensure the comparability of experimental results. The deletion of transcription factors was demonstrated to lower, instead of eliminating the expression of regulated genes (Figure 4B), and rescued the sporulation deficiency (Figure 4A). Interestingly, no significant germination defect was observed in spores of Δ*adeR* Δ*gerAA* mutant with decreased expression of *ald* (Figure 4C). However, spores of Δ*ahrC* Δ*rocR* Δ*gerAA* mutant with low expression of *rocG* showed remarkable germination deficiency (Figure 4C). Moreover, spores of Δ*adeR* Δ*ahrC* Δ*rocR* Δ*gerAA* mutant exhibited similar germination deficiency phenotype with that of Δ*ahrC* Δ*rocR* Δ*gerAA* mutant spores (Figure 4C), indicating that the expression of *rocG*, not *ald*, was essential for ensuring spore quality with normal germination capability. Taken together, these results strongly implied that the RocG-mediated glutamate metabolism regulated both the sporulation efficiency and spore quality likely by energy supply. As for the Ald-mediated alanine metabolism, its effect on sporulation was not likely executed by providing energy sources. Instead, it is more likely associated with premature germination, as quantities of phase-dark spores were observed in the sporulating cells of Δ*ald* mutant (Figure 2A).

Ald inhibits premature germination during sporulation by regulating L-alanine content in the external environment of spores

As mentioned above, the occurrence of phase-dark spores in Δ*ald* mutant drove us to investigate the effect of Ald-mediated alanine metabolism on premature germination. As shown in Figure 5, Δ*ald* mutant generated large amounts of phase-dark spores, and the percentage of phase-bright spores was only 11.5%. However, the deletion of *gerAA* in Δ*ald* mutant significantly raised

the percentage of phase-bright spores to 61.5%, nearly close the wild type (76.5%). In addition, no significant germination deficiency was observed in Δ*ald* Δ*gerAA* spores when compared with wild-type (Figure 5C). Thus, it could conclude that the absence of Ald caused sporulation defect by inducing premature germination during sporulation. In order to identify the period of premature germination occurrence, the sporulation process of Δ*ald* mutant was examined by time-lapse microscopy. Interestingly, two models of premature germination were observed as (i) forespores prematurely germinated during mother cell lysis, and then released; (ii) dormant spores were released, and then induced to premature germination (Figure 5D).

The association of Ald and premature germination raised up an interesting speculation that the interruption of alanine metabolism may lead to the over-accumulation of L-alanine, which triggers premature germination. To test this possibility, *ald* was artificially expressed in Δ*ald* mutant under IPTG-inducible promoter, and the sporulation phenotype as well as the environmental L-alanine content at later sporulation phase (t_{19}) of these mutants were examined. Results showed that the percentage of phase-bright spores gradually increased with elevating the expression level of *ald* (Figure 6A-6C). Notably, the expression of *ald* exhibited a decrease when the concentration of added IPTG increased to1 mM, which was possibly due to the toxicity of IPTG to cells (Figure 6C). In contrast, the opposite trend was observed for environmental L-alanine concentration of Δ*ald* mutant, which reached to 3397.4 μM without IPTG induction, while decreased to wild-type levels of 145.9 μM when > 200 μM IPTG was added to elevate the expression of *ald* (Figure 6B). Consequently, Ald-mediated alanine metabolism was responsible for controlling the L-alanine content in the external environment of spores to prevent premature germination, and thus ensuring proper sporulation.

RocG regulates both the σ^K-dependent spore release and spore

properties by providing energy sources

As indicated above, RocG-mediated glutamate metabolism regulated both sporulation efficiency and spore quality likely by energy supporting. To further investigate this, we first explored the specific sporulation stage interrupted by *rocG* deletion. To this end, we constructed the fusion of *gfp* to the promotor of sporulation stage-specific sigma factors, σ^F, σ^E, σ^G, and σ^K, which regulate polar division, engulfment, spore maturation and spore release, respectively (6, 10, 22, 23). In general, the activation of the specific σ factor can be reflected by the σ-dependent GFP fluorescence, thus visually displaying the impaired sporulation stage (22). Results showed that the activation of σ^F and σ^E in Δ*rocG* mutant were similar with that in wild-type (Figure 7A-7B). As for σ^G, its activation can be achieved in Δ*rocG* mutant although the activation time was delayed (Figure 7C). Notably, although the σ^K-dependent GFP fluorescence in Δ*rocG* mutant appeared properly at t_7, it abnormally existed even until t_{25} (Figure 7D). As σ^K is responsible for regulating the cell wall degrading enzymes, leading to mother cell lysis and spore release (24, 25), its fluorescence is supposed to disappear with spore release. The presence of σ^K-dependent GFP fluorescence at the end of sporulation of Δ*rocG* mutant indicated that its σ^K was activated in the mother cell but failed to regulate mother cell lysis, inferring the impaired spore release process in Δ*rocG* mutant (Figure 7E).

To further understanding the regulating role of RocG in sporulation, *rocG* was artificially expressed in Δ*rocG* mutant under IPTG-inducible promoter. The results showed that the percentage of released spores increased significantly with elevating the expression level of *rocG* (Figure 8A, B). The addition of more than 10 μM IPTG could remarkably improve the percentage of spore release to the wild-type level (Figure 8B). As hypothesized previously, RocG-mediated glutamate metabolism could provide energy sources to drive sporulation proceeding, we then tested the ATP levels in sporulating cells to verify this.

Since previous research has demonstrated that the ATP content of mother cells during sporulation is highest at t_1 (14, 26), we examined ATP content at t_1 in Δ*rocG* mutant with different *rocG* expression levels. Accordingly, the level of ATP in Δ*rocG* mutant increased with elevating the *rocG* expression (Figure 8C). Notably, the ATP content of Δ*rocG* mutant with 50 μM IPTG induction was almost double of the wild type (Figure 8C). Then, we wondered if such high level of ATP in sporulating cells could affect the properties of the future spores. To test this, the spores generated under different concentrations of IPTG induction were purified and examined for the germination phenotypes as well as the DPA content and heat resistance. Interestingly, Δ*rocG* spores with 50 μM IPTG induction showed higher germination efficiency but significantly lower DPA content as well as decreased heat resistance than the wild-type spores (Figure 8D, Figure S3). Taken together, the expression of *rocG* can indeed provide energy support for sporulation, at least the spore release regulated by σ^K, thus contributing to the proper sporulation process. However, exceeded expression of *rocG* can accumulate excessive ATP in sporulating cells, which might adversely affect the spore properties.

DISCUSSION

Sporulation as a typical bacterial differentiation process has been extensively studied for decades, and the morphological events along with the signal transduction for this process are relatively well elucidated (6-10). However, as an energy-consuming process, the sources of energy supply and the underlying regulating mechanism are lack of research. In addition, how the generated spores keep in dormant state during sporulation remains mysterious. Here, we proved that Ald-mediated alanine metabolism decreased the concentration of the typical germinant L-alanine in sporulating environment to a certain level, thus avoiding premature germination and maintaining spore dormancy. Moreover, we also provided evidences supporting that RocG-mediated

glutamate metabolism ensured proper sporulation, especially mother cell lysis, by regulating ATP levels during sporulation. Additionally, excessively high ATP levels during the sporulation process was supposed to adversely affect the properties of the spores produced, including faster germination efficiency, lower DPA content along with decreased heat resistance. Our data revealed that sporulation was a highly orchestrated and exquisite biological process requiring the balance of diverse metabolism pathways, e.g. alanine catabolism to eliminate surrounding germinants, and glutamate metabolism providing appropriate level of energy to ensure both the sporulation completion and high quality of generated spores.

Our finding of alanine catabolism eliminating the germinant L-alanine leads to another open question that which catabolism pathways or biological reactions are responsible for regulating the balance of other germinants during sporulation. Indeed, in *B. cereus* and *B. subtilis* spores, alanine racemases converting the germinant L-alanine to germination inhibitor D-alanine are detected in the coat, thus they can potentially prevent premature germination (27, 28). As for the glutamate metabolism, except for the metabolite ATP, whether other metabolic intermediates are involved in sporulation needs to be further investigated. In fact, the metabolite 2-oxoglutarate can participate in the synthesis of amino acids, nucleotides, and NADH, and thus is able to potentially affect spore formation (29). Finally, since glutamate is a universal amino group donor and commonly exists in all living organisms (30), whether the other spore-forming bacteria also employ glutamate metabolism as the energy sources for sporulation remains an interesting question worth to be further explored.

METHODS

Strains and plasmids

B. subtilis strains used in this study are listed Table S1. Plasmids construction is listed in Table S2, and primers are described in Table S3. For gene replacement strategy, primer pairs were used to amplify the flanking genomic regions of the corresponding gene. PCR products and the respective antibiotic resistance gene were used for Gibson assembly (NEB, USA) (31). The product was used to transform *B. subtilis* PY79 to obtain the mutant allele.

General methods

Sporulation of *B. subtilis* was carried out at 37°C by suspending cells in Schaeffer's liquid medium (Difco Sporulation Medium, DSM) (32). Sporulation t_0 was identified as the third hour after spores suspending in DSM. The percentage of sporulation was evaluated by calculating the ratio of total number of colonies forming units (CFU) before and after heat treatment (80°C, 20 min) (33). The percentage of phase-bright or released spores were counted based on the according phase-contrast images. To ensure confidence of the data, at least 800 cells were counted for each experiment. Spore germination with different germinants was examined as described previously with some modification (14, 34). Briefly, purified spores were heat activated at 75°C for 30 min, and then induced by L-Ala (10 mM) or AGFK (2.5 mM L-Asparagine, 5 mg/mL D-glucose, 5 mg/mL D-fructose, and 50 mM KCl) at 37°C, by DDA (1 mM in 10 mM Tris-HCl, pH 7.4) at 42°C. The germination was tested by determining the DPA release as descried in the following text.

Spore purification

Matured spores were purified as described previously (14). Briefly, 22 hrs DSM culture was centrifuged and washed 3 times by DDW and then kept in 4°C with constant agitation. The suspension was washed once a day and resuspended in DDW. After 7 days, the suspension was centrifuged to collect the pellet. 20%

379 histodenz solution was used to resuspend the pellet at a ratio of 400 μL per 10
380 mL of DSM for 30 min on ice. Aliquots (200 μL) of resuspension mixture were
381 then added on top of 900 μL 50% histodenz solution, and gradient fractionation
382 was carried out by centrifugation at 15,000 rpm at 4°C for 30 min. The pellet
383 was collected and washed at least 5 times by DDW. Phase contrast microscopy
384 was then used to evaluate the purity of pellet spores. Spores with >99% purity
385 can be used for following experiments, otherwise the purification steps should
386 be carried out more than once.
387
388 **Tandem Mass Tag-based (TMT) quantitative proteomics analysis**
389
390 TMT quantitative proteomics analysis was carried out between pure dormant
391 spores (DS) and vegetative cells (VC) at sporulation t_0 by APTBIO (Shanghai,
392 China). DS and VC samples were collected by centrifugation and then freeze-
393 dried and bead-grinded using FastPrep-24 (M. P. Biomedicals, LLC, USA).
394 Samples were then extracted for proteins and performed the proteomics
395 analysis by LC-MS/MS system. A statistical analysis was performed using a t-
396 test to determine the significance (p-value) of differentially-expressed proteins.
397 The expression level of proteins with $p < 0.05$ and fold change > 1.2 (the
398 expression level increased by more than 1.2-fold or decreased by less than
399 0.83-fold) were considered as significant difference.
400
401 **DPA measurements**
402
403 DPA release was detected as described previously with some modifications
404 (35). Briefly, spore germination was induced by L-Ala, AGFK or DDA at 37°C or
405 42°C in a 96-well plate. Spores (OD_{600} of 10), 10 mM germinants, 25 mM K-
406 Hepes buffer (pH 7.4) as well as 50 mM $TbCl_3$ were mixed in 200 μL and Tb^{3+}-
407 DPA fluorescence intensity was monitored at Ex/Em = 270/545 nm by a TECAN
408 Spark 10M microplate reader (TECAN, Switzerland). Total DPA content of

409 spores were evaluated by boiling the spores (OD_{600} of 1) for 20 min and mixing
410 the spores and 50 mM $TbCl_3$ to 200 µL in a 96-well plate. The DPA standard
411 solution was serially diluted and detected together to obtain a standard curve.
412 The detection parameters for DPA release were the same as above, and the
413 total DPA content of spores was calculated based on the standard curve.
414
415 **Phase-contrast and fluorescence microscopy**
416
417 Phase-contrast and fluorescence microscopy were performed using a Nikon
418 DS-Qi2 microscope equipped with a Nikon Ph3 DL 100x/1.25 Oil phase contrast
419 objective. Both bacterial cells (500 µL) and spores (50 µL) were centrifuged,
420 and the pellets were resuspended with 5 ~ 10 µL PBSx1 and then imaged on
421 the pad. For fluorescence imaging, 1,000 ms exposure time was required for
422 GFP. For time-lapse imaging of sporulation, Imaging System Cell Chamber
423 (AttofluorTM Cell Chamber) was used. Sporulating cells were collected at the
424 late sporulation stage by centrifugation and imaged on a DSM gel-pad with 1%
425 agarose at 37°C. Image analysis and processing were performed by ImageJ2.
426
427 **Real-Time Quantitative PCR (RT-qPCR)**
428
429 Real-time quantitative PCR (RT-qPCR) was carried out followed the protocol
430 described previously (14). RNA samples of sporulating cells (500 µL) were
431 collected from DSM by centrifugation, and then extracted by FastPure
432 Cell/Tissue Total RNA Isolation Kit V2 (Vazyme Biotech Co..Ltd). HiScript III All
433 in-one RT SuperMix for qPCR (Vazyme Biotech Co..Ltd) was used to reverse
434 transcribed RNA samples. RT-qPCR reactions were conducted with
435 PerfectStart Green qPCR SuperMix (TransGen Biotech Co., Ltd). CFX Connect
436 RealTime PCR Dection System (Bio-Rad) was used to detect the fluorescence
437 and *scr* gene that has unchangeable expression level during sporulation was
438 selected to normalize sample data. Each sample was detected in triplicate and

at least three independent measurements were conducted.

Environmental L-alanine content assay

Measurement of environmental L-Alanine level was performed as the instruction of Amplite Fluorimetric L-Alanine Assay Kit (AAT Bioquest, Inc.). DSM media of sporulating cells at indicated timepoints was collected from the supernatant after centrifugation. The fluorescence intensity of L-Alanine in DSM media was monitored by TECAN Spark 10M microplate reader (TECAN, Switzerland) at Ex/Em = 540/590 nm. The standard solution of L-alanine was serially diluted and detected together to obtain a standard curve, and the L-Alanine content in the environment was calculated based on the standard curve.

ATP content assay

Measurement of ATP content in mother cell was performed using the BacTiter-Glo Microbial Cell Viability Assay (Promega). As guided by the instructions, sporulating cells in DSM at t_1 were collected and detected luminescence using a TECAN Spark 10M microplate reader (TECAN, Switzerland). The standard solution of ATP was serially diluted and detected together to obtain a standard curve and the ATP level was calculated based on the standard curve.

Data processing

Unless stated otherwise, each experiment was carried out at least three times. GraphPad Prism 8 software was used for all statistical analysis, data processing, and graph drawing. One-way ANOVA was performed to analyze the variance and $p < 0.05$ was regarded as significance for all data statistics.

ACKNOWLEDGEMENTS

We are grateful to Dr. Bing Zhou (The Hebrew University of Jerusalem) for valuable discussions and comments. This work was supported by National Natural Science Foundation of China (NSFC) (grant No. 32372470), NSFC (grant No. 32001658), Agricultural Research Outstanding Talents of China (grant No. 13210317) awarded to Lei Rao, and 2115 Talent Development Program of China Agricultural University. The authors declare no conflicts of interest.

478 **REFERENCES**

479

480 (1) Driks A. 2002. Maximum shields: the assembly and function of the bacterial
481 spore coat. *Trends Microbiol.* 10:251-254.
482 (2) Stragier P. Losick R. 1996. Molecular genetics of sporulation in *Bacillus*
483 *subtilis*. *Annu. Rev. Genet.* 30:297-241.
484 (3) Nicholson W L, Munakata N, Horneck G, Melosh H J. Setlow P. 2000.
485 Resistance of *Bacillus* endospores to extreme terrestrial and extraterrestrial
486 environments. *Microbiol. Mol. Biol. Rev.* 64:548-572.
487 (4) Setlow P. 2006. Spores of *Bacillus subtilis*: their resistance to and killing by
488 radiation, heat and chemicals. *J. Appl. Microbiol.* 101:514-525.
489 (5) Vreeland R H, Rosenzweig W D. Powers D W. 2000. Isolation of a 250
490 million-year-old halotolerant bacterium from a primary salt crystal. *Nature*
491 407:897-900.
492 (6) Riley E P, Schwarz C, Derman A I. Lopez-Garrido J. 2020. Milestones in
493 *Bacillus subtilis* sporulation research. *Microb Cell* 8:1-16.
494 (7) Tokuyasu K. Yamada E. 1959. Fine Structure of *Bacillus subtilis*: II.
495 Sporulation Progress. *The Journal of Cell Biology* 5:129-133.
496 (8) Kawata T, Inoue T. Takagi A. 1963. Electron microscopy of spore formation
497 and germination in *Bacillus subtilis*. *Jpn. J. Microbiol.* 7:23-41.
498 (9) Piggot P. Coote J. 1976. Genetic aspects of bacterial endospore formation.
499 *Bacteriol. Rev.* 40:908-962.
500 (10) Errington J. 2003. Regulation of endospore formation in *Bacillus subtilis*.
501 *Nat. Rev. Microbiol.* 1:117-126.
502 (11) Phillips Z. Strauch M. 2002. *Bacillus subtilis* sporulation and stationary
503 phase gene expression. *Cell. Mol. Life Sci.* 59:392-402.
504 (12) Charba J. Nakata H. 1977. Role of glutamate in the sporogenesis of
505 *Bacillus cereus*. *J. Bacteriol.* 130:242-248.
506 (13) Siranosian K J, Ireton K. Grossman A D. 1993. Alanine dehydrogenase
507 (ald) is required for normal sporulation in *Bacillus subtilis*. *J. Bacteriol.*

175:6789-6796.

(14) Rao L, Zhou B, Serruya R, Moussaieff A, Sinai L. Ben-Yehuda S. 2022. Glutamate catabolism during sporulation determines the success of the future spore germination. *iScience* 25:105242.

(15) Driks A. 2002. Overview: development in bacteria: spore formation in *Bacillus subtilis*. *Cell. Mol. Life Sci.* 59:389-391.

(16) Ramírez‐Guadiana F H, Meeske A J, Wang X, Rodrigues C D. Rudner D Z. 2017. The *Bacillus subtilis* germinant receptor GerA triggers premature germination in response to morphological defects during sporulation. *Mol. Microbiol.* 105:689-704.

(17) Gao Y, Barajas-Ornelas R D C, Amon J D, Ramírez-Guadiana F H, Alon A, Brock K P, Marks D S, Kruse A C. Rudner D Z. 2022. The SpoVA membrane complex is required for dipicolinic acid import during sporulation and export during germination. *Genes Dev.* 36:634-646.

(18) Belitsky B R. Sonenshein A L. 1998. Role and regulation of *Bacillus subtilis* glutamate dehydrogenase genes. *J. Bacteriol.* 180:6298-6305.

(19) Yoshida K, Fujita Y. Ehrlich S D. 1999. Three asparagine synthetase genes of *Bacillus subtilis*. *J. Bacteriol.* 181:6081-6091.

(20) de Vries Y P, Atmadja R D, Hornstra L M, de Vos W M. Abee T. 2005. Influence of glutamate on growth, sporulation, and spore properties of *Bacillus cereus* ATCC 14579 in defined medium. *Appl. Environ. Microbiol.* 71:3248-3254.

(21) Lin T H, Wei G T, Su C C. Shaw G C. 2012. AdeR, a PucR-type transcription factor, activates expression of L-alanine dehydrogenase and is required for sporulation of *Bacillus subtilis*. *J. Bacteriol.* 194:4995-5001.

(22) Meeske A J, Rodrigues C D, Brady J, Lim H C, Bernhardt T G. Rudner D Z. 2016. High-throughput genetic screens identify a large and diverse collection of new sporulation genes in *Bacillus subtilis*. *PLoS Biol.* 14:e1002341.

(23) Hilbert D W. Piggot P J. 2004. Compartmentalization of gene expression during *Bacillus subtilis* spore formation. *Microbiol. Mol. Biol. Rev.* 68:234-262.

(24) Nugroho F A, Yamamoto H, Kobayashi Y. Sekiguchi J. 1999.

538 Characterization of a new sigma-K-dependent peptidoglycan hydrolase gene
539 that plays a role in *Bacillus subtilis* mother cell lysis. *J. Bacteriol.* 181:6230-
540 6237.
541 (25) Smith T J. Foster S J. 1995. Characterization of the involvement of two
542 compensatory autolysins in mother cell lysis during sporulation of *Bacillus*
543 *subtilis* 168. *J. Bacteriol.* 177:3855-3862.
544 (26) Updegrove T B, Harke J, Anantharaman V, Yang J, Gopalan N,
545 Wu D, Piszczek G, Stevenson D M, Amador-Noguez D. Wang J D. 2021.
546 Reformulation of an extant ATPase active site to mimic ancestral GTPase
547 activity reveals a nucleotide base requirement for function. *elife* 10:e65845.
548 (27) Stewart B T. Halvorson H O. 1953. Studies on the spores of aerobic
549 bacteria I: the occurrence of alanine racemase. *J. Bacteriol.* 65:160-166.
550 (28) Yasuda Y, Kanda K, Nishioka S, Tanimoto Y, Kato C, Saito A,
551 Fukuchi S, Nakanishi Y. Tochikubo K. 1993. Regulation of L-alanine-initiated
552 germination of *Bacillus subtilis* spores by alanine racemase. *Amino Acids* 4:89-
553 99.
554 (29) Huergo L F. Dixon R. 2015. The emergence of 2-oxoglutarate as a master
555 regulator metabolite. *Microbiol. Mol. Biol. Rev.* 79:419-435.
556 (30) Gundlach J, Commichau F M. Stülke J. 2018. Perspective of ions and
557 messengers: an intricate link between potassium, glutamate, and cyclic di-AMP.
558 *Curr. Genet.* 64:191-195.
559 (31) Guérout-Fleury A-M, Frandsen N. Stragier P. 1996. Plasmids for ectopic
560 integration in *Bacillus subtilis*. *Gene* 180:57-61.
561 (32) Harwood C R. Cutting S M. *Molecular biological methods for Bacillus*;
562 Chichester ; New York : Wiley, 1990.
563 (33) Zhou B, Semanjski M, Orlovetskie N, Bhattacharya S, Alon S,
564 Argaman L, Jarrous N, Zhang Y, Macek B, Sinai L. Ben-Yehuda S. 2019.
565 Arginine dephosphorylation propels spore germination in bacteria. *Proc. Natl.*
566 *Acad. Sci. USA* 116:14228-14237.
567 (34) Vepachedu V R. Setlow P. 2007. Role of SpoVA proteins in release of

568 dipicolinic acid during germination of *Bacillus subtilis* spores triggered by
569 dodecylamine or lysozyme. *J. Bacteriol.* 189:1565-1572.
570 (35) Yi X. Setlow P. 2010. Studies of the commitment step in the germination of
571 spores of *Bacillus* species. *J. Bacteriol.* 192:3424-3433.
572

573 **Figure legends**

574

575 **Figure 1.** TMT quantitative proteomic analysis. (A) Proteins were compared
576 between dormant spores (DS) and vegetative cells (VC) of at the onset of
577 sporulation (T_0); (B) Heatmap of differential expression of proteins in DS
578 samples were grouped using Hierarchical Cluster Analysis. Each line
579 represented a protein, with FC > 1.2 and $p < 0.05$ (T-test) as the screening
580 criteria. The proteins with significantly decreased expression were marked in
581 blue, the proteins with significantly increased expression were in red, the
582 proteins without quantitative information were in gray; (C) The volcano map of
583 proteins in DS group was drawn based on two factors of fold change (FC) of
584 differential expression and the P value of T test. The proteins with significantly
585 decreased expression (FC < 0.83, $p < 0.05$) were marked in blue, the proteins
586 with significantly increased expression (FC > 1.2, $p < 0.05$) were in red, and the
587 non-differentiated proteins were in gray; (D) The enrichment map (Top 20) of
588 KEGG pathway enrichment analysis of differentially expressed proteins in the
589 DS group by Fisher's exact test. The color of the bubble represents the
590 significance of the enriched KEGG pathway, and the color gradient represents
591 the size of the P-value (-log10), and the closer to red, the smaller the P-value.
592 The size of the bubble represents the amount of differential protein.

593

594 **Figure 2.** Alanine and glutamate metabolism co-regulate sporulation with an
595 additive effect. (A) Phase-contrast images of sporulating cells at the late
596 sporulation stage t_{19}. *B. subtilis* PY79 (wt), YZ11 (Δ*ald*), YZ19 (Δ*rocG*), YZ12
597 (Δ*ald* Δ*rocG*) and YZ13 (Δ*ald* Δ*rocG*, *amyE::ald-rocG*) strains were induced to
598 sporulate in DSM at 37°C for 22 hrs and followed by microscopy. Images
599 captured from a representative experiment out of three independent biological
600 repeats. Scale bar, 2 μm; (B) The percentage of sporulation of the strains
601 described in (A). Data are presented as the percentage of total number of
602 colonies forming units (CFU) before and after heat treatment (80°C, 20 min).

603 Shown are average values and SD obtained from three independent biological
604 repeats.
605
606 **Figure 3.** RocG-mediated glutamate metabolism is essential for ensuring the
607 sporulation efficiency. (A) Phase-contrast images of sporulating cells at the late
608 sporulation stage t_{19}. *B. subtilis* PY79 (wt), YZ22 (Δ*ald* Δ*rocG* Δ*gerAA*), YZ24
609 (Δ*ald* Δ*rocG* Δ*gerAA, amyE::P*$_{IPTG}$*-rocG*), YZ25 (Δ*ald* Δ*rocG* Δ*gerAA,*
610 *amyE::P*$_{IPTG}$*-ald*) and YZ26 (Δ*ald* Δ*rocG* Δ*gerAA, amyE::P*$_{IPTG}$*-rocG-ald*) strains
611 were induced to sporulate in DSM at 37°C for 22 hrs and followed by
612 microscopy. 50 μM IPTG was added to the YZ24, YZ25 and YZ26 cultures at
613 the sporulation t_0 to induce corresponding gene expression. Images captured
614 from a representative experiment out of three independent biological repeats.
615 Scale bar, 2 μm; (B) Quantification of the experiment described in (A). Data are
616 presented as percentages of the number of the phase-bright spores and all
617 sporulating cells in the same image. Shown are average values and SD
618 obtained from three independent biological repeats (n ≥ 800 for each strain);
619 (C) Spores of wt, as well as YZ24, YZ25 and YZ26 strains with 50 μM IPTG
620 induction, were incubated with AGFK (10 mM) to trigger germination. DPA
621 release was measured by detecting the relative fluorescence units (RFU) of
622 Tb^{3+}-DPA. Shown is a representative experiment out of three independent
623 biological repeats.
624
625 **Figure 4.** The expression of *rocG* is significant to the quality of correspondingly
626 generated spores. (A) Phase-contrast images of sporulating cells at the late
627 sporulation stage t19. *B. subtilis* PY79 (wt), YZ81 (Δ*adeR* Δ*gerAA*), YZ23
628 (Δ*ahrC* Δ*rocR* Δ*gerAA*) and YZ90 (Δ*adeR* Δ*ahrC* Δ*rocR* Δ*gerAA*) strains were
629 induced to sporulate in DSM at 37°C for 22 hrs and followed by microscopy.
630 Images captured from a representative experiment out of three independent
631 biological repeats. Scale bar, 2 μm; (B) Expression of the *ald* gene in wt, YZ11

(Δ*ald*) and YZ81 strains, and *rocG* gene in wt, YZ19 (Δ*rocG*) and YZ23 strains; (C) Spores of wt, YZ81, YZ23 and YZ90 strains were incubated with AGFK (10 mM) to trigger germination. DPA release was measured by detecting the relative fluorescence units (RFU) of Tb^{3+}-DPA. Shown is a representative experiment out of three independent biological repeats.

Figure 5. The absence of Ald induces premature germination during sporulation. (A) Phase-contrast images of sporulating cells at the late sporulation stage t_{19}. *B. subtilis* PY79 (wt), YZ11 (Δ*ald*) and YZ21 (Δ*ald* Δ*gerAA*) strains were induced to sporulate in DSM at 37°C for 22 hrs and followed by microscopy. Images captured from a representative experiment out of three independent biological repeats. Scale bar, 2 μm; (B) Quantification of the experiment described in (A). Data are presented as percentages of the number of the phase-bright spores and all sporulating cells in the same image. Shown are average values and SD obtained from three independent biological repeats (n ≥ 800 for each strain); (C) Spores of wt, YZ11 and YZ21 strains were incubated with AGFK (10 mM) to trigger germination. DPA release was measured by detecting the relative fluorescence units (RFU) of Tb^{3+}-DPA. Shown is a representative experiment out of three independent biological repeats. (D) Models of the premature germination in Δ*ald* mutant. YZ11 strain was induced to sporulate in DSM at 37°C. After 14 hrs of incubation, spores were collected on a DSM gel-pad, and followed by time-lapse microscopy at a 10 min interval.

Figure 6. Ald-mediated alanine metabolism regulates L-alanine content in the external environment of spores. (A) Phase-contrast images of sporulating cells at the late sporulation stage t_{19}. YZ31 (Δ*ald, amyE::*P_{IPTG}*-ald*) strains were induced to sporulate in DSM at 37°C for 22 hrs and followed by microscopy. 0-1000 μM IPTG was added at the sporulation t_0 to induce *ald* expression. Images captured from a representative experiment out of three independent biological repeats. Scale bar, 2 μm; (B) The percentage of phase-bright spores as well as

662 the environmental L-alanine content of the wt and YZ31 strains described in (A).
663 The percentage of phase-bright spores are presented as ratio of the number of
664 the phase-bright spores and all sporulating cells in the same image (n ≥ 800 for
665 each strain). The environmental L-alanine content was evaluated at the end of
666 sporulation; (C) Expression of the *ald* gene in YZ31 strains described in (A).
667 Shown are average values and SD obtained from three independent biological
668 repeats.
669
670 **Figure 7.** Cytological sporulation assay reveals the impaired sporulation stage
671 of Δ*rocG* mutants. (A-D) Phase contrast and the indicated fluorescent images
672 of wt and YZ19 (Δ*rocG*) cells harboring four transcriptional fusions, σ^F, σ^E, σ^G
673 and σ^K, at sporulation t_2, $t_{2.5}$, t_4 and t_{25}, t_7 and t_{25}, respectively. Images captured
674 from a representative experiment out of three independent biological repeats.
675 Scale bar, 2 μm; (E) Models of the sporulation defect in Δ*rocG* mutants.
676
677 **Figure 8.** RocG regulates both spore release and spore properties. (A) Phase-
678 contrast images of sporulating cells at the late sporulation stage t_{19}. *B. subtilis*
679 PY79 (wt), YZ19 (Δ*rocG*) and YZ32 (Δ*rocG, amyE::*P_{IPTG}*-rocG*) strains were
680 induced to sporulate in DSM at 37°C for 22 hrs and followed by microscopy. 0-
681 50 μM IPTG was added to YZ32 at the sporulation t_0 to induce *rocG* expression.
682 Images captured from a representative experiment out of three independent
683 biological repeats. Scale bar, 2 μm; (B) Quantification of the experiment
684 described in (A). Data are presented as percentages of the number of the
685 released spores and all sporulating cells in the same image. Shown are
686 average values and SD obtained from three independent biological repeats (n
687 ≥ 800 for each strain); (C) Strains indicated in (A) were grown in DSM
688 sporulation medium. IPTG was added to the YZ32 cultures at the t_0 to induce
689 *rocG* expression. The DSM cultures were collected at t_1 and analyzed for ATP
690 level. Shown are average values and SD obtained from three independent
691 biological repeats. (D) Spores of wt and YZ32 strains with different IPTG

692 induction were incubated with (i) L-alanine (10 mM), (ii) AGFK (10 mM) and (iii)
693 DDA (10 mM) to trigger germination. Total DPA content (iv) of these spores were
694 measured by boiling for 20 min. DPA release was measured by detecting the
695 relative fluorescence units (RFU) of Tb^{3+}-DPA. Shown is a representative
696 experiment out of three independent biological repeats.
697

Figure 1

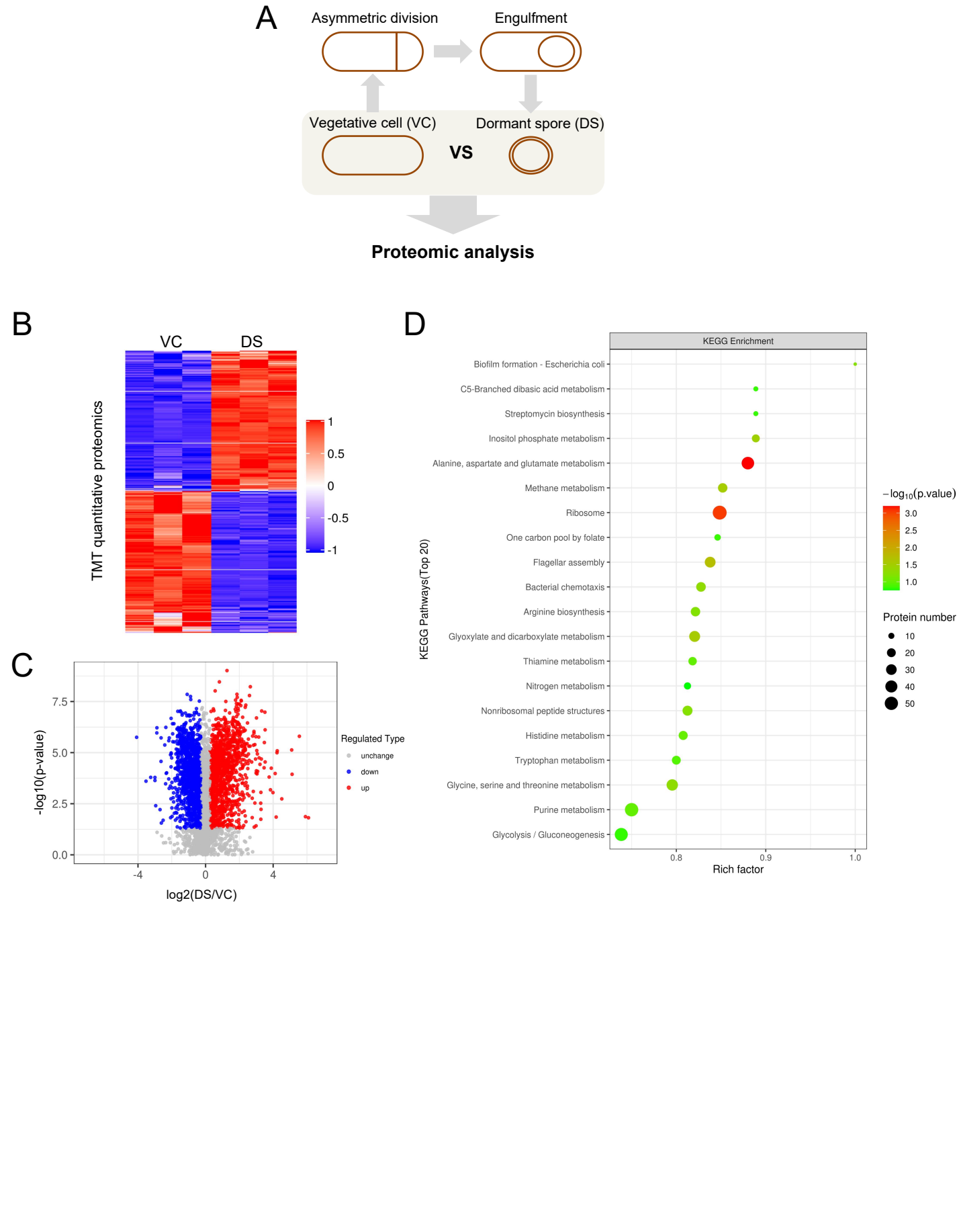
A
Asymmetric division
Engulfment
Vegetative cell (VC)
Dormant spore (DS)
VS
Proteomic analysis
B
VC
DS
TMT quantitative proteomics
1
0.5
0
-0.5
-1
C
-log10(p-value)
log2(DS/VC)
Regulated Type
unchange
down
up
D
KEGG Enrichment
KEGG Pathways(Top 20)
Biofilm formation - Escherichia coli
C5-Branched dibasic acid metabolism
Streptomycin biosynthesis
Inositol phosphate metabolism
Alanine, aspartate and glutamate metabolism
Methane metabolism
Ribosome
One carbon pool by folate
Flagellar assembly
Bacterial chemotaxis
Arginine biosynthesis
Glyoxylate and dicarboxylate metabolism
Thiamine metabolism
Nitrogen metabolism
Nonribosomal peptide structures
Histidine metabolism
Tryptophan metabolism
Glycine, serine and threonine metabolism
Purine metabolism
Glycolysis / Gluconeogenesis
Rich factor
−log10(p.value)
Protein number

Figure 2

A

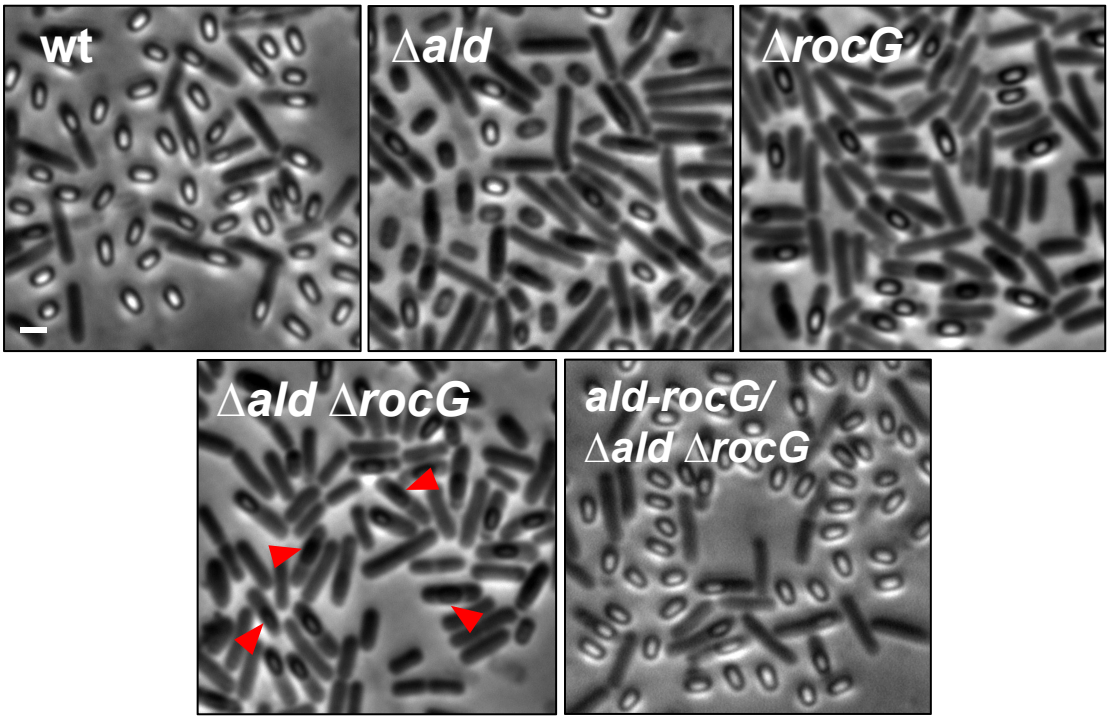
wt
Δald
ΔrocG
Δald ΔrocG
ald-rocG/
Δald ΔrocG

B

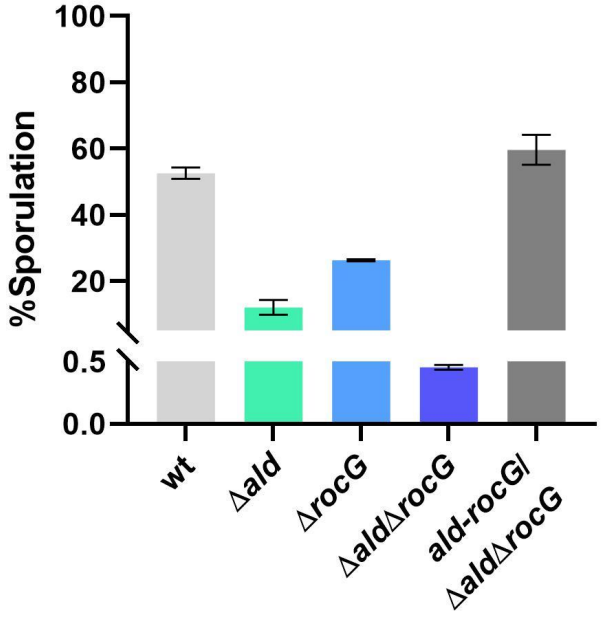
%Sporulation
100
80
60
40
20
0.5
0.0
wt
Δald
ΔrocG
ΔaldΔrocG
ald-rocG/
ΔaldΔrocG

Figure 3

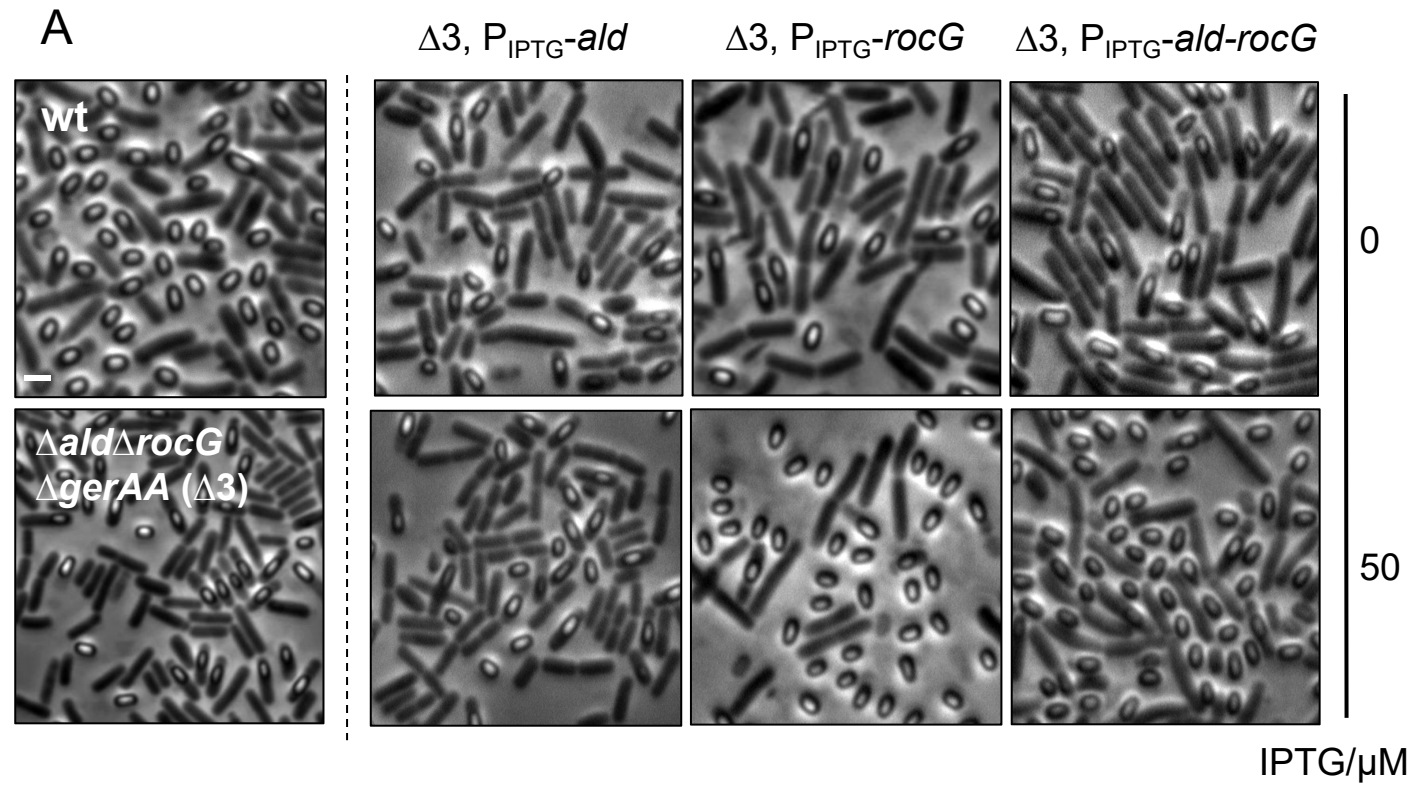
A
Δ3, P_IPTG-ald
Δ3, P_IPTG-rocG
Δ3, P_IPTG-ald-rocG
wt
ΔaldΔrocG
ΔgerAA (Δ3)
0
50
IPTG/μM

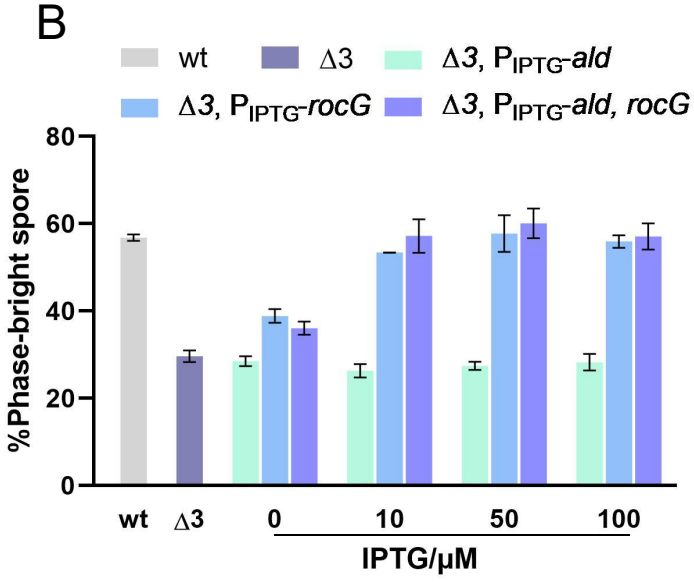
B
wt
Δ3
Δ3, P_IPTG-ald
Δ3, P_IPTG-rocG
Δ3, P_IPTG-ald, rocG
%Phase-bright spore
0
20
40
60
80
wt
Δ3
0
10
50
100
IPTG/μM

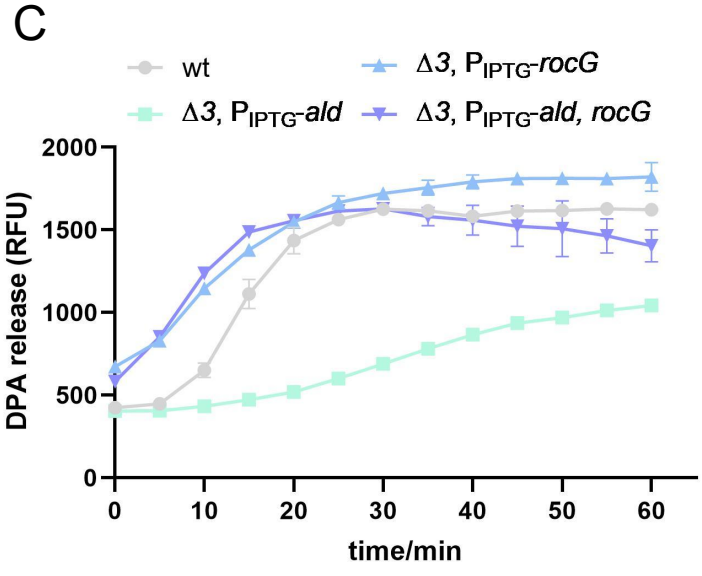
C
wt
Δ3, P_IPTG-rocG
Δ3, P_IPTG-ald
Δ3, P_IPTG-ald, rocG
DPA release (RFU)
0
500
1000
1500
2000
0
10
20
30
40
50
60
time/min

Figure 4

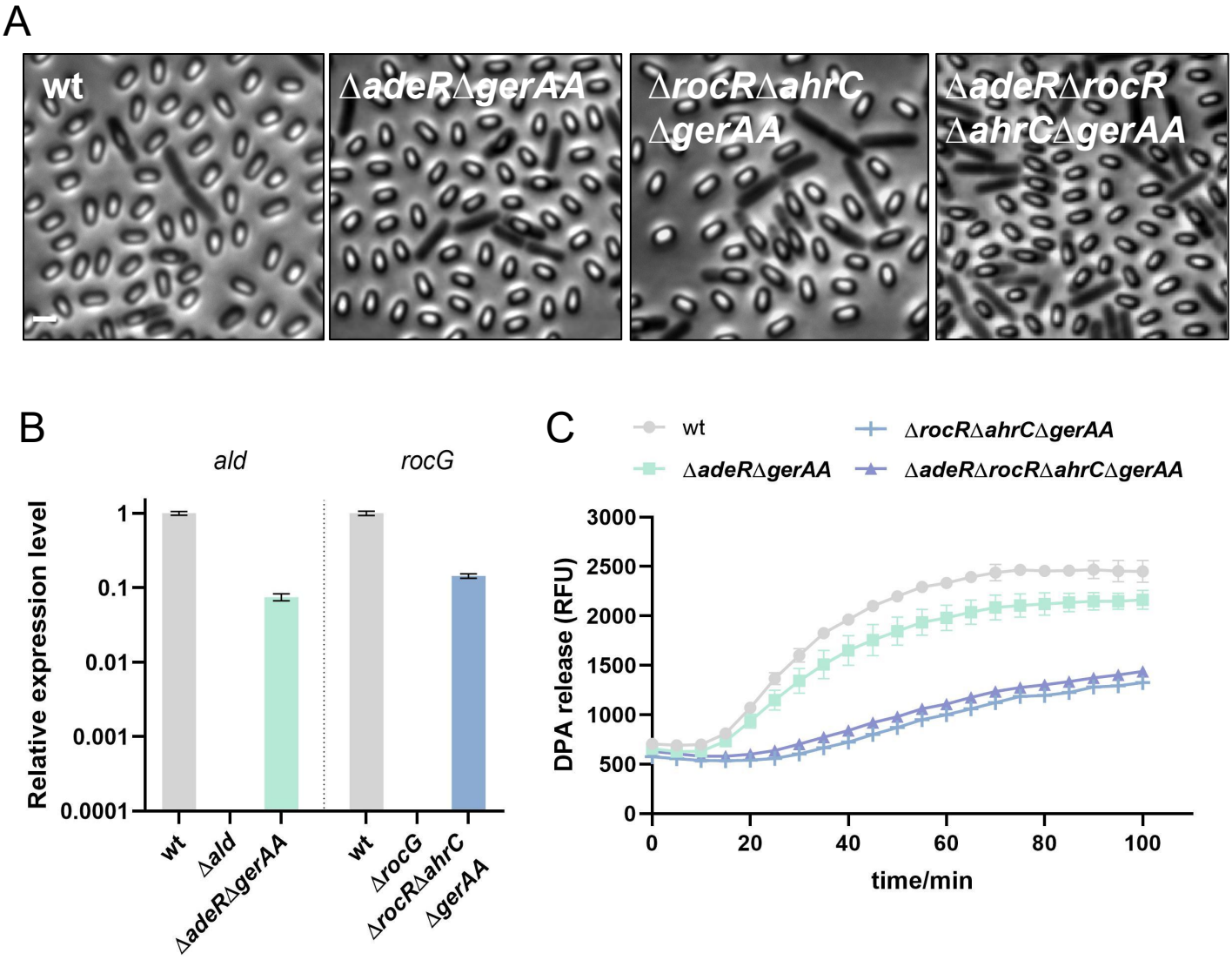
A
wt
ΔadeRΔgerAA
ΔrocRΔahrC ΔgerAA
ΔadeRΔrocR ΔahrCΔgerAA
B
ald
rocG
Relative expression level
1
0.1
0.01
0.001
0.0001
wt
Δald
ΔadeRΔgerAA
wt
ΔrocG
ΔrocRΔahrC ΔgerAA
C
wt
ΔrocRΔahrCΔgerAA
ΔadeRΔgerAA
ΔadeRΔrocRΔahrCΔgerAA
DPA release (RFU)
3000
2500
2000
1500
1000
500
0
0
20
40
60
80
100
time/min

Figure 5

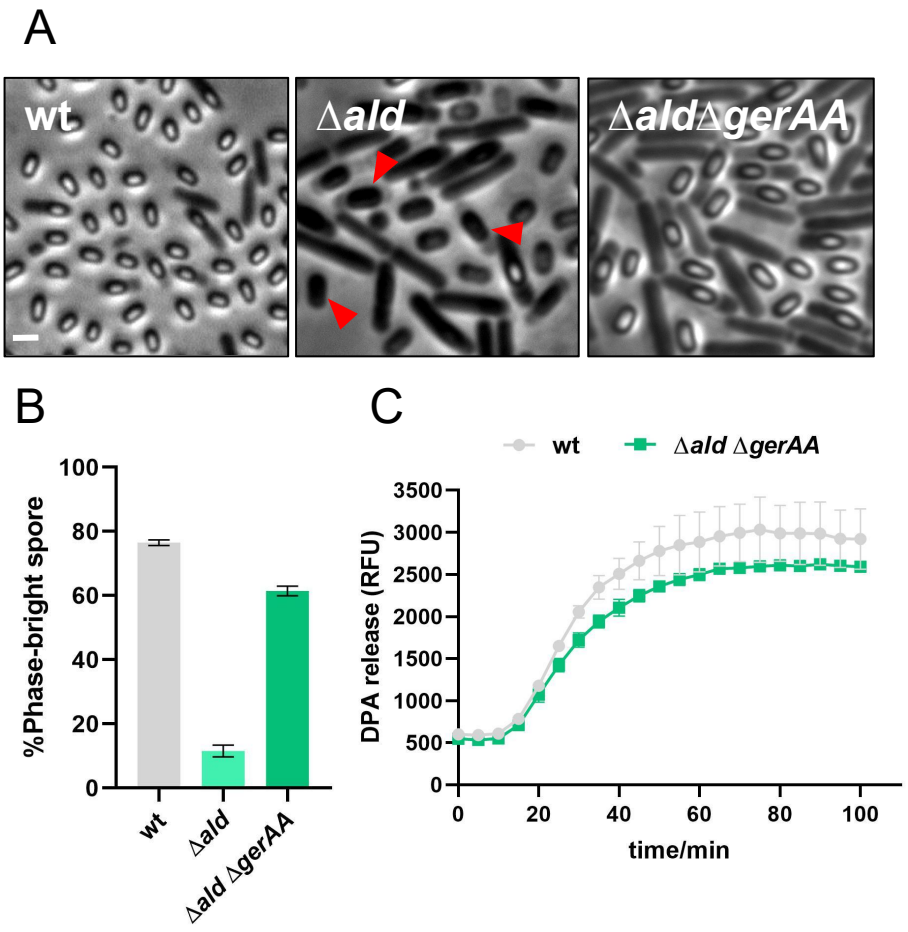
A
wt
Δald
ΔaldΔgerAA
B
%Phase-bright spore
100
80
60
40
20
0
wt
Δald
Δald ΔgerAA
C
wt
Δald ΔgerAA
DPA release (RFU)
3500
3000
2500
2000
1500
1000
500
0
0
20
40
60
80
100
time/min
D
Δald
(i) Mother cell lysis
(ii) Spore release
Germinated spore release
Spore premature germination

Figure 6

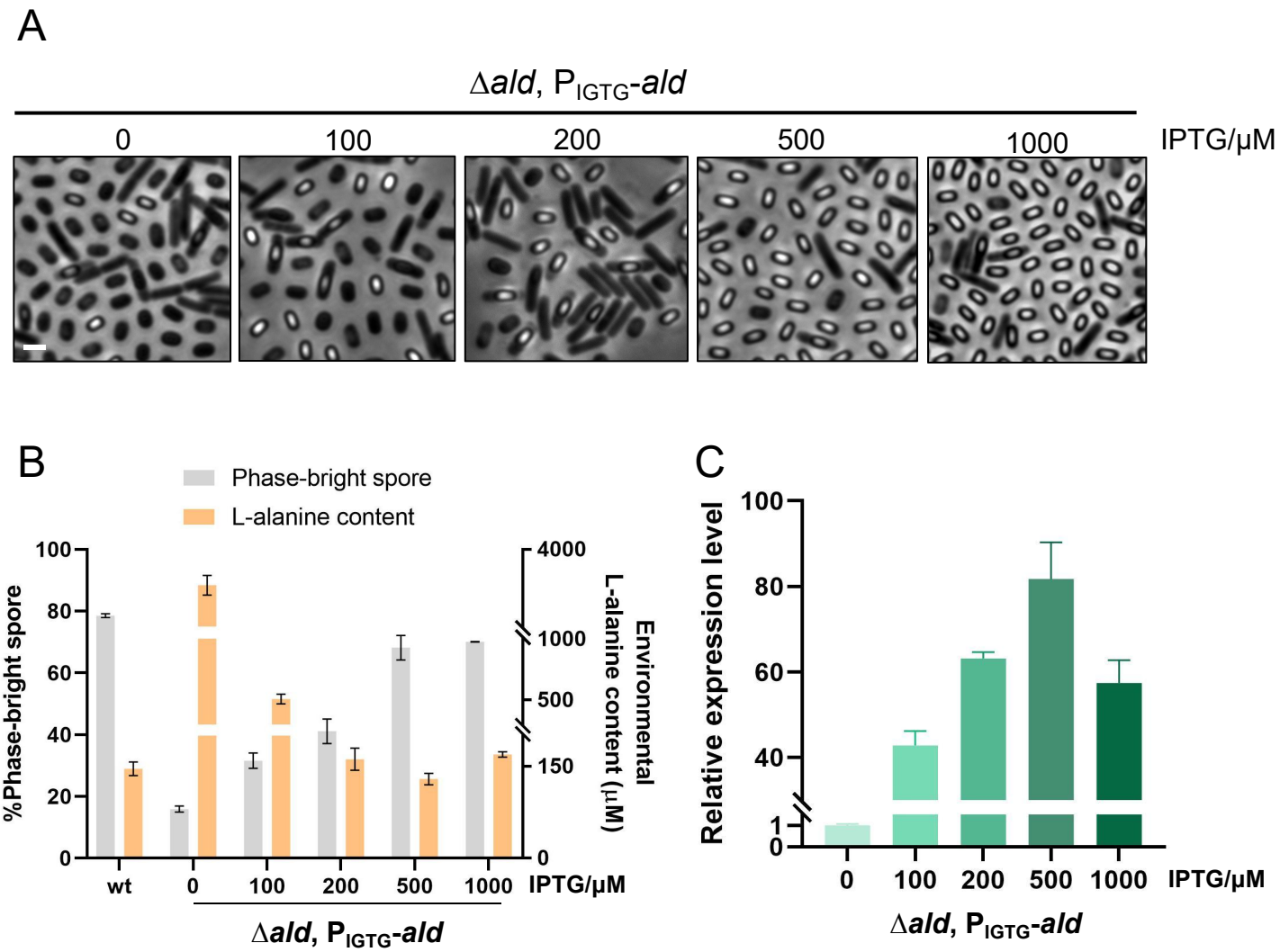
A
Δald, P IGTG-ald
0
100
200
500
1000
IPTG/μM
B
Phase-bright spore
L-alanine content
%Phase-bright spore
Environmental L-alanine content (μM)
wt
0
100
200
500
1000
IPTG/μM
Δald, P IGTG-ald
C
Relative expression level
0
100
200
500
1000
IPTG/μM
Δald, P IGTG-ald

Figure 7

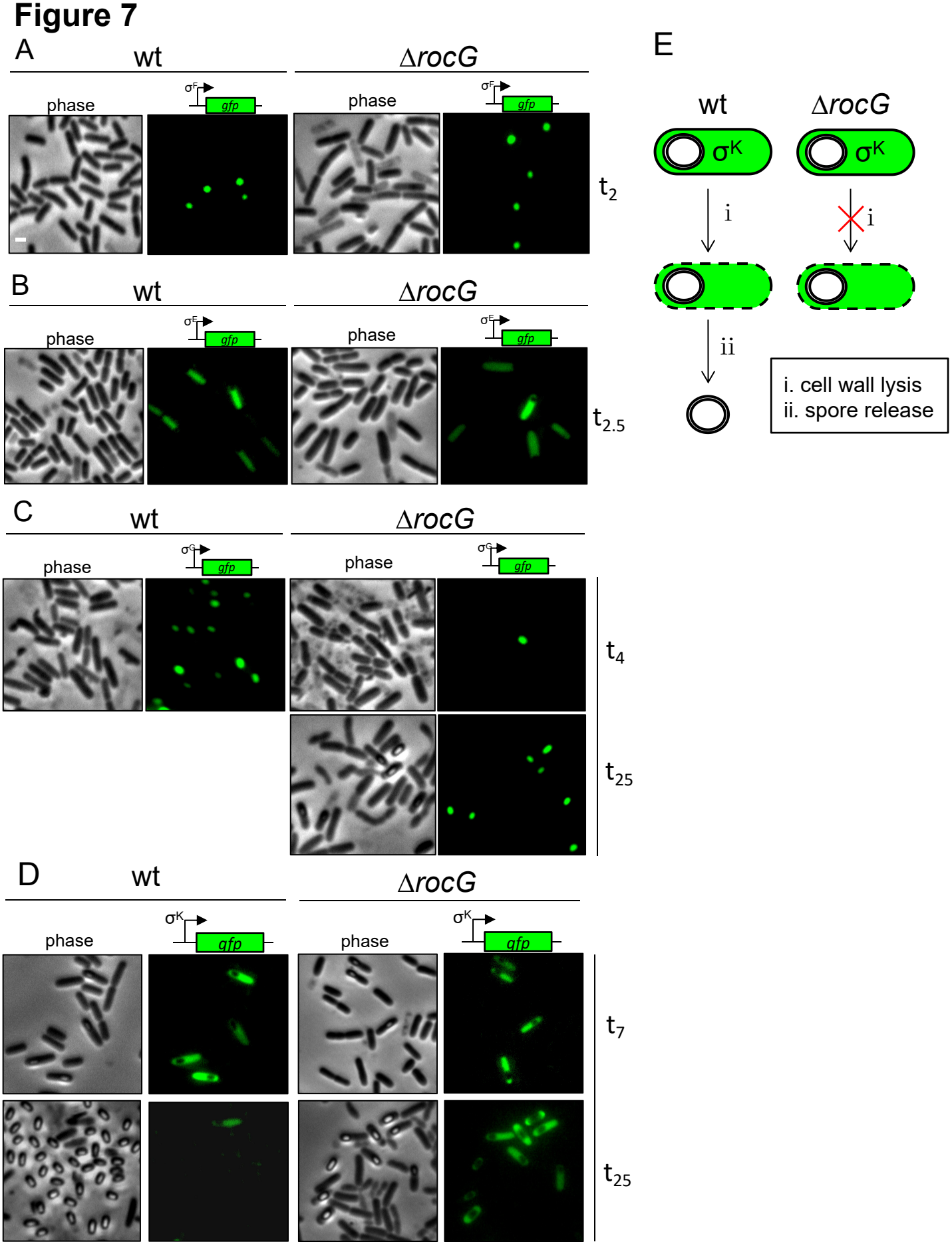
A
wt
ΔrocG
phase
σF
gfp
t2
B
wt
ΔrocG
phase
σF
gfp
t2.5
C
wt
ΔrocG
phase
σG
gfp
t4
t25
D
wt
ΔrocG
phase
σK
gfp
t7
t25
E
wt
ΔrocG
σK
i
ii
i. cell wall lysis
ii. spore release

Figure 8

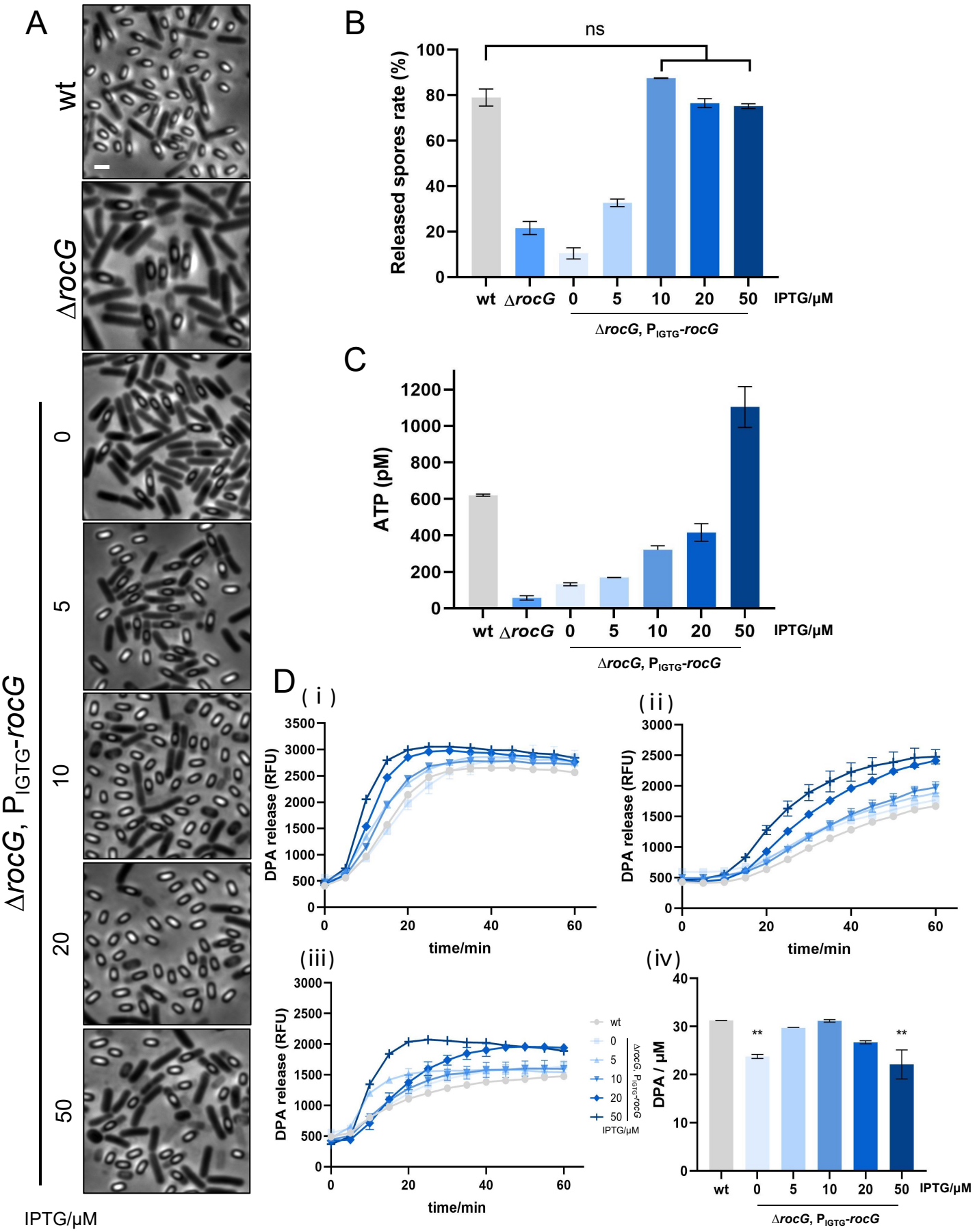
A
wt
ΔrocG
ΔrocG, PIGTG-rocG
0
5
10
20
50
IPTG/μM
B
ns
Released spores rate (%)
100
80
60
40
20
0
wt
ΔrocG
0
5
10
20
50
IPTG/μM
ΔrocG, PIGTG-rocG
C
ATP (pM)
1200
1000
800
600
400
200
0
wt
ΔrocG
0
5
10
20
50
IPTG/μM
ΔrocG, PIGTG-rocG
D
(i)
DPA release (RFU)
time/min
(ii)
DPA release (RFU)
time/min
(iii)
DPA release (RFU)
time/min
wt
0
5
10
20
50
ΔrocG, PIGTG-rocG
IPTG/μM
(iv)
DPA / μM
**
**
wt
0
5
10
20
50
IPTG/μM
ΔrocG, PIGTG-rocG